

THE OFFICIAL MAGAZINE OF THE OCEANOGRAPHY SOCIETY

Oceanography

CITATION

Girton, J.B., B.S. Chinn, and M.H. Alford. 2011. Internal wave climates of the Philippine Seas. *Oceanography* 24(1):100–111, doi:10.5670/oceanog.2011.07.

COPYRIGHT

This article has been published in *Oceanography*, Volume 24, Number 1, a quarterly journal of The Oceanography Society. Copyright 2011 by The Oceanography Society. All rights reserved.

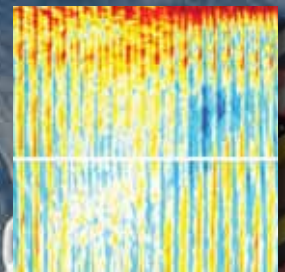
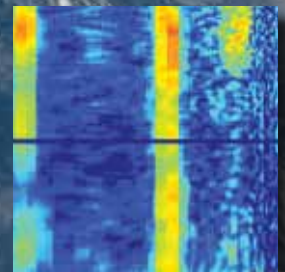
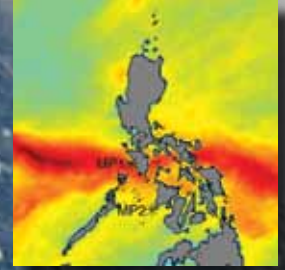
USAGE

Permission is granted to copy this article for use in teaching and research. Republication, systematic reproduction, or collective redistribution of any portion of this article by photocopy machine, reposting, or other means is permitted only with the approval of The Oceanography Society. Send all correspondence to: info@tos.org or The Oceanography Society, PO Box 1931, Rockville, MD 20849-1931, USA.

BY JAMES B. GIRTON, BRIAN S. CHINN,
AND MATTHEW H. ALFORD

Internal Wave Climates of the Philippine Seas

ABSTRACT. Internal wave measurements from moorings and profiling floats throughout the Philippine Archipelago, collected as part of the Office of Naval Research Philippine Straits Dynamics Experiment, reveal a wealth of subsurface processes, some of which have not been observed previously (in the Philippines or elsewhere). Complex bathymetry and spatially varying tide and wind forcing produce distinct internal wave environments within the network of seas and channels, ranging from quiescent interior basins to remotely forced straits. Internal tides in both the diurnal and semidiurnal bands dominate much of the velocity structure and are likely the dominant source of energy for mixing in the region. In addition, the transfer of energy from the internal tide directly to near-inertial motions through parametric subharmonic instability appears to be active and, rather than wind forcing, is the dominant source of near-inertial band energy.





INTRODUCTION

The Philippine Archipelago is a complex network of islands and basins with inter-connecting straits and sills (Figure 1). Substantial differences in water-column structure appear among the different basins due to the varying mixtures of source waters from the South China Sea (SCS) and Pacific Ocean, varying local inputs of heat and freshwater from sun and rain at the surface, and differing exchange rates and residence times (the times over which weaker mixing processes can act). Barotropic (depth-independent) tidal flows through many of the passages are quite strong, reflecting substantial tidal surface height differences between the Pacific and SCS as well as acceleration through topographic constrictions.

A component of the Office of Naval Research (ONR) Philippine Straits Dynamics Experiment (PhilEx) was devoted to the exploration of small-scale oceanic processes, including internal waves (primarily internal tides and near-inertial waves) and their influence on turbulence and mixing. Knowledge of these processes is important not only to the general understanding of how archipelagos influence internal wave dynamics but also to understanding their specific impact on the currents, stratification, and nutrient distribution of the Philippine seas. For example, are surface current fluctuations dominated by barotropic or internal tides? Are internal waves a significant contributor to the mixing that supplies nutrients to the upper-ocean ecosystem and maintains oxygen levels in the deep waters? Or, does the inhibition of internal waves create an environment distinct from the open ocean? How much is the interocean

exchange of thermocline waters affected by internal wave modulated mixing?

Many of these questions can only be answered by combining localized measurements of internal waves and turbulence with appropriately calibrated numerical models to extrapolate over the broader region. Thus, in addition to the PhilEx observational program, a suite of numerical models using a variety of resolutions and forcing mechanisms were run (Arango et al., 2011; Hurlburt et al., 2011; Lermusiaux et al., 2011; May et al., 2011). Some of them included tidal and wind forcing at appropriate spatial and temporal scales to generate internal waves; some of the largest known internal tide sources (in the southern Sulu Sea and northern South China Sea) clearly show radiating waves (Zhang et al., 2010). Simulating internal waves that can be directly compared to observations, however, involves considerable challenges (most obviously due to the resolution required), and it has not yet proven feasible to simulate the wave fields of the interior Philippine seas. The measurements described here suggest ways that this simulation might be accomplished.

This paper first presents a review of the properties of internal waves and the physical mechanisms responsible for their generation and dissipation. Next, we describe the PhilEx measurement program, and provide an overview of the rich internal wave field recorded by the experiment's moored and drifting platforms. Particular attention is paid to the "near-inertial" band—the low-frequency limit of the internal wave range that is often strongly correlated with wind forcing. In the Philippines, this correlation is curiously absent, requiring the consideration of more exotic dynamical

processes. Finally, we interpret the salient features of the PhilEx region through their connections to the regional barotropic-tide and wind-forcing functions, together with the influence of the basin and strait geometry on remotely generated internal wave energy.

frequency—the natural response to vertical perturbations in a stratified fluid. This period is usually 10 minutes or longer (compared to just a few seconds for the most energetic surface waves). The slowest internal waves are influenced by Earth’s rotation, with the

shallower water. Thus, internal waves carry energy and momentum from the surface to the bottom of the ocean, and vice versa, to drive turbulence, mixing, and currents when they dissipate at the opposite boundary or ocean interior. Because linear internal waves exist in a moving ocean, they can also be advected by the mean flow, particularly when comparable to the group speed of the wave. This advection can result in wave steepening in converging flow or prevention of wave signals traveling through straits with a mean flow.

“MANY OF THESE QUESTIONS CAN ONLY BE ANSWERED BY COMBINING LOCALIZED MEASUREMENTS OF INTERNAL WAVES AND TURBULENCE WITH APPROPRIATELY CALIBRATED NUMERICAL MODELS TO EXTRAPOLATE OVER THE BROADER REGION.”

WAVES BELOW THE SURFACE

Just as disturbances of the air-sea interface can propagate as surface waves, disturbances within the water column of a stratified fluid can propagate as internal waves. When the density interfaces and currents are strong, these waves may become nonlinear solitons, propagating horizontally for long distances with coherent wave fronts visible in satellite imagery (Jackson et al., 2011). More generally, however, propagating wave solutions to the linear equations of fluid motion exist over a range of scales (roughly 10 m to 100 km) and frequencies (from μHz to mHz ; see Figure 2). The specific limits of this “internal wave range” are set by the bathymetry, forcing mechanism, density stratification, and Earth’s rotation.

Because the density contrasts within the water column are much weaker than those between the water and air, internal waves exist in slow motion, with the shortest periods set by the buoyancy

longest periods in the internal wave range set by the inertial (or Coriolis) frequency—the natural response to horizontal perturbations—corresponding to a period of 12 hours at the north or south pole, two to three days in the Philippines, and increasingly large values approaching the equator.

In a continuously stratified fluid, internal waves can propagate vertically as well as horizontally, with energy traveling along sloping ray paths determined by their frequency. On contact with the ocean bottom, internal waves reflect, preserving their propagation slope, with enhanced concentration of energy when the topographic slope is close to the propagation slope (“critical reflection”) or waves propagate into

Internal Tides

The large-scale gravitational forcing of the moon and sun drive surface height variations and predominantly *barotropic* (i.e., depth-uniform) currents. In the presence of stratification and bottom slope, these tidal currents can drive vertical motions that then propagate as internal waves with depth-varying structure, in turn influencing the currents and stratification both through their own fluctuating motions and through the net influence of mixing as they break or dissipate. For weak-to-moderate levels of forcing, these “internal tides” retain the frequency and sinusoidal shape of the generating barotropic (surface) tide but can be distinguished by their variation with depth. When currents and stratification become strong enough, the internal tide may steepen and break up into nonlinear trains of short-wavelength solitons with time scales approaching

James B. Girton (girton@apl.washington.edu) is *Affiliate Assistant Professor, Applied Physics Laboratory, University of Washington, Seattle, WA, USA*. **Brian S. Chinn** is *PhD Candidate, Applied Physics Laboratory, University of Washington, Seattle, WA, USA*. **Matthew H. Alford** is *Senior Oceanographer and Associate Professor, Applied Physics Laboratory, University of Washington, Seattle, WA, USA*.

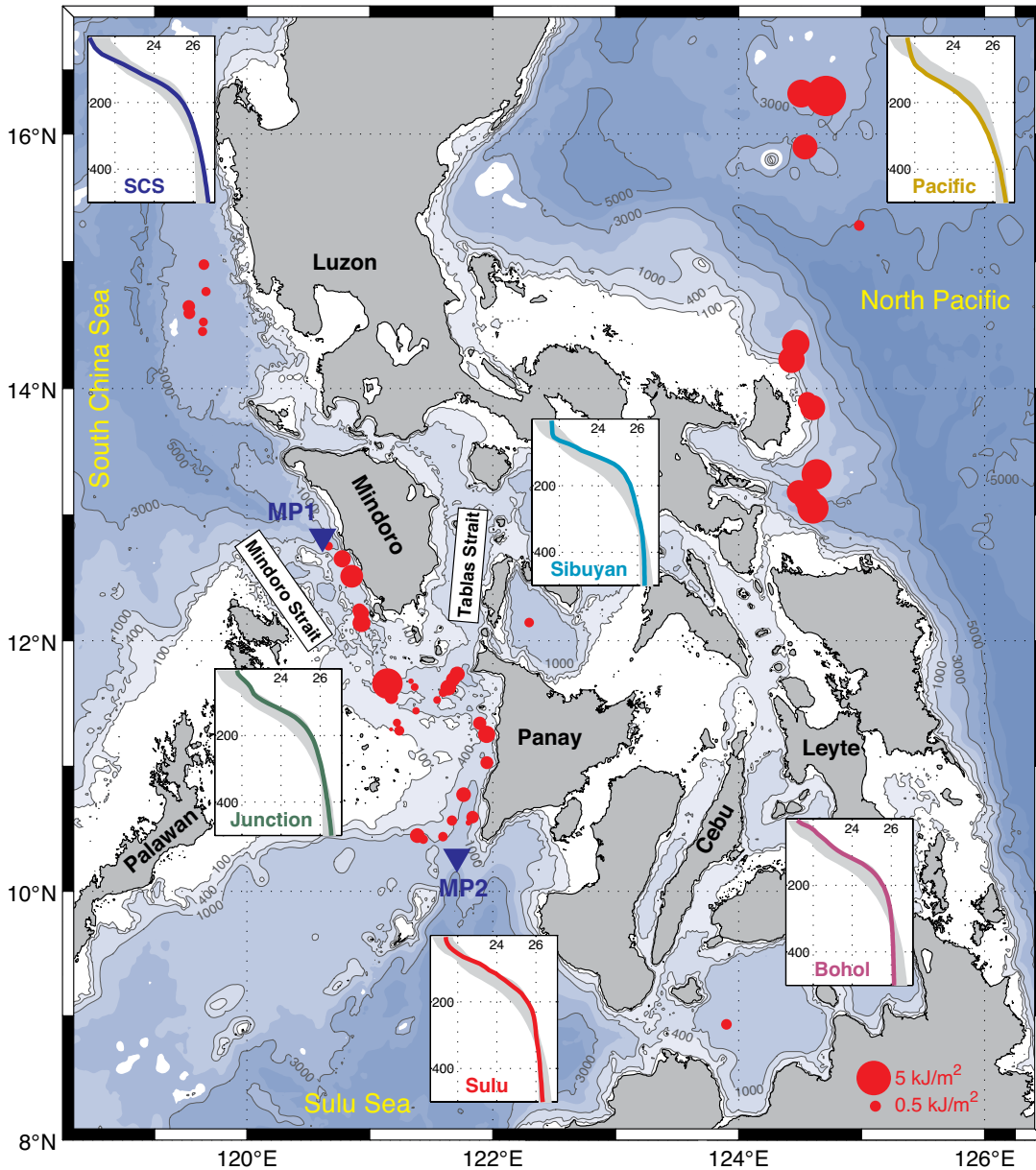


Figure 1. Chart of the Philippine Archipelago, showing the location of McLane Labs moored profilers (MPs 1 and 2; blue triangles) and internal-tide-available potential energy (APE) from EM-APEX profiling float measurements (red dots). Bathymetric contours from SRTM30_PLUS (Becker et al., 2009) are labeled in meters, with additional shaded contours at 1000-m intervals. Inset panels show the mean stratification (potential density, σ_θ , profiles measured by EM-APEX in different regions of the archipelago, with the same envelope of mean profiles shaded gray in each panel.

the minimum for internal waves (Jackson et al., 2011). This breakup can occur either at the generation site or along the propagation pathway (Zhao and Alford, 2006).

Near-Inertial Waves

In addition to tides, the other major generator of oceanic internal waves is wind variability. Because wind variations occur at all frequencies, with the

most energetic variations occurring in the synoptic, or weather, band between two- and 10-day periods, wind-driven internal waves tend to be largest near their lower limit—the inertial frequency. While much work has been done on the generation and propagation of near-inertial internal waves in the open ocean, less is known about the near-inertial band in constricted straits and isolated basins. Because near-inertial waves have longer

horizontal wavelengths than higher-frequency internal waves, the presence of steep topography makes free-wave solutions less likely, although topographically trapped or standing-wave modes are still possible.

Internal Wave Climate

Internal waves may be locally or remotely generated and live for hours to weeks, depending on their dissipation

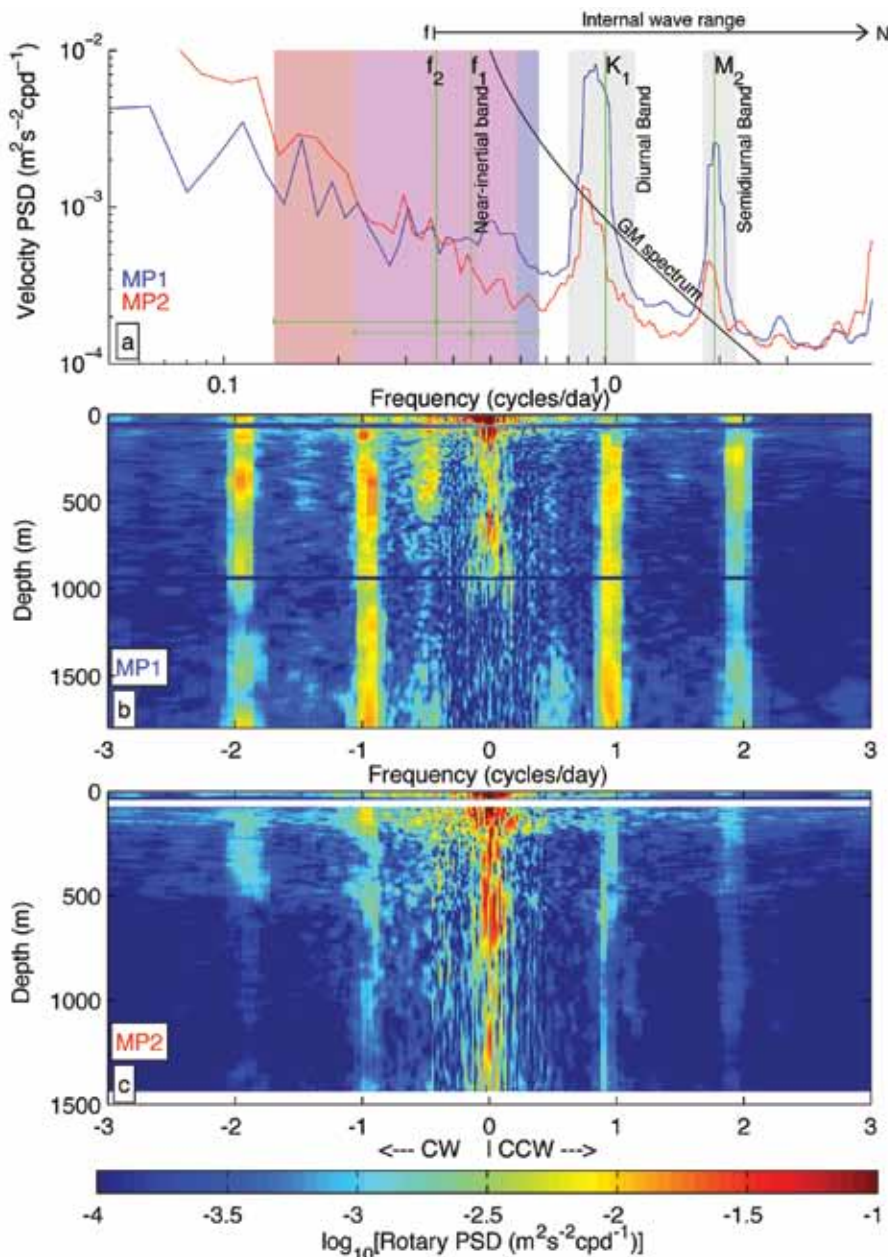


Figure 2. (a) Vertically averaged frequency spectra from MP1 and MP2, showing excess tidal and inertial-band energy at MP1 and stronger low-frequency motions at MP2. The inertial frequency at the two moorings is indicated by the green lines labeled “ f_1 ” and “ f_2 ,” as are the frequencies of the dominant diurnal (K_1) and semidiurnal (M_2) tidal components. (b,c) Rotary frequency spectra vs. depth at MP1 (b) and MP2 (c), with positive frequencies indicating counterclockwise rotation with time and negative indicating clockwise. At MP1, the inertial peak is dominantly clockwise, as expected, in the upper water column, but nearly linearly polarized (equal CW and CCW energy) close to the bottom. At MP2, tides are weaker and less barotropic, but low-frequency mesoscale variability extends throughout the water column.

rate. Dissipation depends on a wide variety of fluid processes, most involving an energy cascade from large to small scales of motion and often driven by flow instability and nonlinear wave-wave interactions. In the intermediate range between vertical scales of ten to several hundred meters in the open ocean, the cascade is made up of a broadband continuum of internal waves, while in shallow shelf and strait regions, the direct influence of turbulence generated by bottom shear or buoyant exchange flows can be important. In the near-surface layer, additional processes are present (with or without topography).

In the open ocean below the surface layer, the combination of intermittent generation processes, long propagation times, and weak interactions among waves acts to produce a “background” internal wave field with a fairly universal frequency and wavenumber spectral structure (Garrett and Munk, 1975). Much of the scientific literature on internal waves, particularly with regard to mixing, assumes this structure. Whether the assumptions and universal shape still hold true within an archipelago, however, is not at all clear.

We begin to approach this issue by characterizing regional “internal wave climates”—that is, the sum of the various wave signals present—through frequency and wavenumber spectra. The net effect of the generation, propagation, and reflection of many waves is a substantial variation among regions with different geometries, including the open ocean, enclosed seas, and constricted passages. This variation is further enhanced by the differences in stratification among the regions (Figure 1) through its influence on wave propagation and

the effectiveness and vertical structure of generation. The stratification itself is largely determined by topography, with a primary influence being the depth of connecting sills between the basins, allowing buoyant exchanges or dense overflows.

Our observations in the Philippines bear out this separation, with energy levels highest in the open basins with large regions of generation or constricted straits connected to them, and lowest in isolated basins with little local generation and little opportunity for incoming waves.

HIGH-RESOLUTION MEASUREMENTS

The observation of internal waves requires sufficient temporal and spatial resolution—ideally resolving vertical wavelengths of 10 m or shorter and the time scales of the dominant forcing, which may include inertial motions (two-day periods in the Philippines), diurnal (24-hour) or semidiurnal (12-hour) tides, or higher-frequency phenomena. These resolutions are not always possible with standard oceanographic surveying techniques. Hence, in addition to the standard shipboard, mooring, and modeling tools, the PhilEx experiment included specialized moored and autonomous instruments optimized for internal waves.

Moored Profilers

A major advance in our ability to characterize internal waves has come with the recent development of vertically profiling moorings. By sampling continuously as the instruments move up and down (driven by buoyancy changes, wave action, an automated winch at the

top or bottom of the mooring, or an internal motor that causes the package to crawl along the wire), it is possible to make measurements with both very high vertical resolution and a temporal resolution sufficient to resolve internal wave time scales.

Two moorings holding wire-crawling McLane Labs moored profilers (MMP) were deployed in PhilEx in the channels adjacent to Mindoro and Panay islands (Figure 1), with the goals of characterizing the internal wave environments and distinguishing between radiating locally generated and incoming remotely generated internal waves. Each crawler carried a conductivity-temperature-depth sensor (CTD) and an acoustic travel time current meter built by Falmouth Scientific Inc., with all instruments recording rapidly enough for meter-scale vertical resolution or better. The northern mooring site (MP1) was in a steep-walled canyon between Apo Reef and Mindoro Island, connecting Mindoro Strait to the South China Sea. Two crawlers were placed on the same mooring (one above the other, with a stop in between), and each made profiles through half of the 1800-m deep water column every three hours. This sampling rate was sufficient to resolve semidiurnal (12-hour) and longer periods. The southern mooring (MP2) was located in 1500 m of water at the entrance to the Sulu Sea, between Panay Island and the Cuyo group. In this shallower location, resolving the semidiurnal tide was possible with a single crawler.

With the new level of detail observed by the MMP, advanced signal processing techniques can be applied over either depth or time. Bandpass filters around the semidiurnal, diurnal, and inertial

frequencies (shaded bands in Figure 2) are useful ways to compare the time-depth structure of the different varieties of internal waves. We expect the different frequency components to be somewhat independent because of their different forcing functions, as well as the predominantly linear nature of internal waves. A particularly informative technique for internal waves is the construction of rotary spectra (e.g., Figure 2b,c), which decompose a vector time or depth series into clockwise and counterclockwise rotating components (by frequency or vertical wavenumber). A key use of rotary spectra is in the study of near-inertial motions (the low-frequency end of the internal wave range), which are predominantly clockwise in the Northern Hemisphere because of the action of the Coriolis force to the right of the velocity vector. The combination of this clockwise rotation in time with the vertical propagation characteristics of internal waves implies that upward- and downward-going energy can be identified by counterclockwise and clockwise rotation with depth, respectively.

The two mooring locations observed dramatically different levels of internal wave activity (Figure 2a), so we will focus mainly on the higher-level location (MP1). Figures 3 and 4 show the along-channel component of velocity at MP1 in raw and filtered forms, illustrating the variety of internal wave structures present. These structures will be discussed further below.

Both moorings were also equipped with upward-looking acoustic Doppler current profilers (ADCP), recording the velocity profile of the top 80 m every minute in order to capture any large-amplitude nonlinear internal waves

(solitons) that might pass by. No clear signatures of such waves were seen at either mooring, however.

Profiling Floats

To complement the fixed measurements of the moorings, a set of Teledyne Webb Research EM-APEX autonomous profiling floats with electromagnetic velocity sensors (Sanford et al., 2007) were deployed and recovered in several locations around the Philippines during

the experiment. Like the moored crawlers, the floats profiled vertically with 5-m resolution, making round trips generally every three hours (again, short enough to resolve the semidiurnal tides but attenuating higher frequencies). Rather than remaining in one place, however, the EM-APEX drifts with the horizontal currents, allowing for spatial sampling. This motion creates the additional challenge of separating temporal and spatial variations in interpreting

the data. We accomplish this separation using the band-limited nature of internal waves: variations over less than one inertial period (two to three days) are treated as temporal, while lower frequencies are interpreted as spatial variability. This approach is likely to be successful as long as the waves' wavelengths are much longer than the float's tidal excursion distance, and the waves' phase speeds are much faster than the float's subtidal drift speed. In the extreme cases of tidal and low-frequency flows accelerating through narrow constrictions, the assumptions are clearly violated, but this situation is rare in our measurements.

The red dots in Figure 1 show the spatial distribution of internal wave energy observed by the EM-APEX. Short-duration harmonic fits to isopycnal displacements by both diurnal and semidiurnal tides were converted to available potential energy (APE) using the mean stratification profile, integrated over the upper 500 m, and smoothed over a two-day window. These measurements illustrate the range of internal tide levels present in the Philippines. APE values are small in the relatively isolated basins of the Sibuyan and Bohol seas (the isolation further emphasized by these basins' weak stratification below 200 m). In contrast, the open Pacific Ocean has large APE values, likely reflecting a combination of locally and remotely generated internal tides. The straits connecting the South China and Sulu seas (Mindoro Strait and the so-called "mixing bowl" at the junction of Mindoro and Tablas straits) were a particular focus of the PhilEx experiment, and so a number of float measurements were made in this region. The complexity of the region is evident

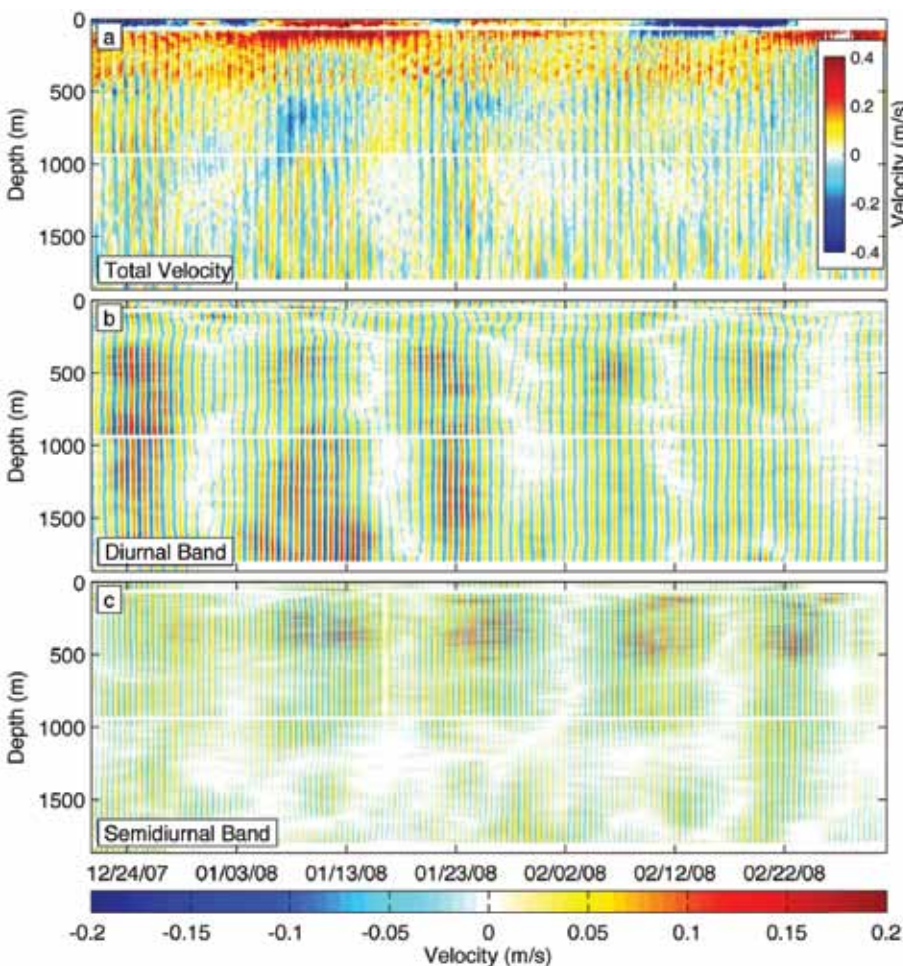


Figure 3. MP1 along-channel currents vs. time and depth, illustrating the wealth of internal wave signals. (a) Unfiltered along-channel velocity from the two moored profilers and near-surface acoustic Doppler current profiler (ADCP), separated by horizontal white bands at 80-m and 900-m depth. (b,c) Bandpass-filtered velocity in the diurnal (b) and semidiurnal (c) bands shaded in Figure 2a. Note that the fortnightly (~ 14-day) spring-neap modulation of the diurnal and semidiurnal bands starts out in phase, as expected near the winter solstice, and is nearly out of phase (expected for the spring equinox) by the end of the record.

in the large variability in internal tide APE, with large and small values in close proximity. Some of this variability could be related to the sampling of different stages of the spring-neap cycle, but a clear pattern of fortnightly modulation is not evident in the APE values. Rather, the variations appear to be related to a complex array of internal tide generation and dissipation locations, with the added possibility of seasonal variations due to stratification and mean flow changes.

WAVES UPON WAVES

The currents and stratification recorded by the moored profilers reveal an intimidating temporal and spatial complexity (Figures 2–4). Both internal wave and low-frequency variations in the currents and stratification are apparent in the unfiltered velocity data (Figure 3), and significant differences between the two mooring sites are clearly evident. Depth-averaged frequency spectra at the two sites (Figure 2a) show that MP1 contains more energy at internal wave frequencies and MP2 contains more low-frequency variability. Nevertheless, both spectra include strong peaks in both the diurnal and semidiurnal bands, much of which is internal tide (as indicated by the structure with depth in Figure 2b,c). Both spectra also contain significantly less near-inertial energy than predicted by the canonical Garrett-Munk (GM) spectrum (Garrett and Munk, 1975). Nevertheless, due to the separation of the inertial and tidal frequencies at this latitude, near-inertial energy can clearly be seen at both sites in certain depth ranges (with enhanced energy at -0.5 cpd frequency, in Figure 2b,c, indicating clockwise rotating currents).

Perhaps the most obvious feature in

the unfiltered currents is a low-frequency modulation of the high-frequency variability with a period close to 14 days. This variability is typical of the tidal spring-neap cycle, reflecting the beating (alternating constructive and destructive interference) of lunar and solar gravitational forcing. Indeed, the tidal (diurnal and semidiurnal) bandpass-filtered time series in Figure 3b,c show this fortnightly variability even more strongly, and with different phasing in the two bands, as

expected from the astronomical forcing.

What is not expected, however, is a fortnightly cycle in the near-inertial bandpass-filtered velocities (Figure 4a). Strong near-inertial variability appears in two distinct depth layers at MP1, and each has a clear signal of low-frequency modulation. Near-inertial currents in the shallower layer centered at 400–500 m show a “checkerboard” pattern, indicating both upward and downward propagating energy. These signals are

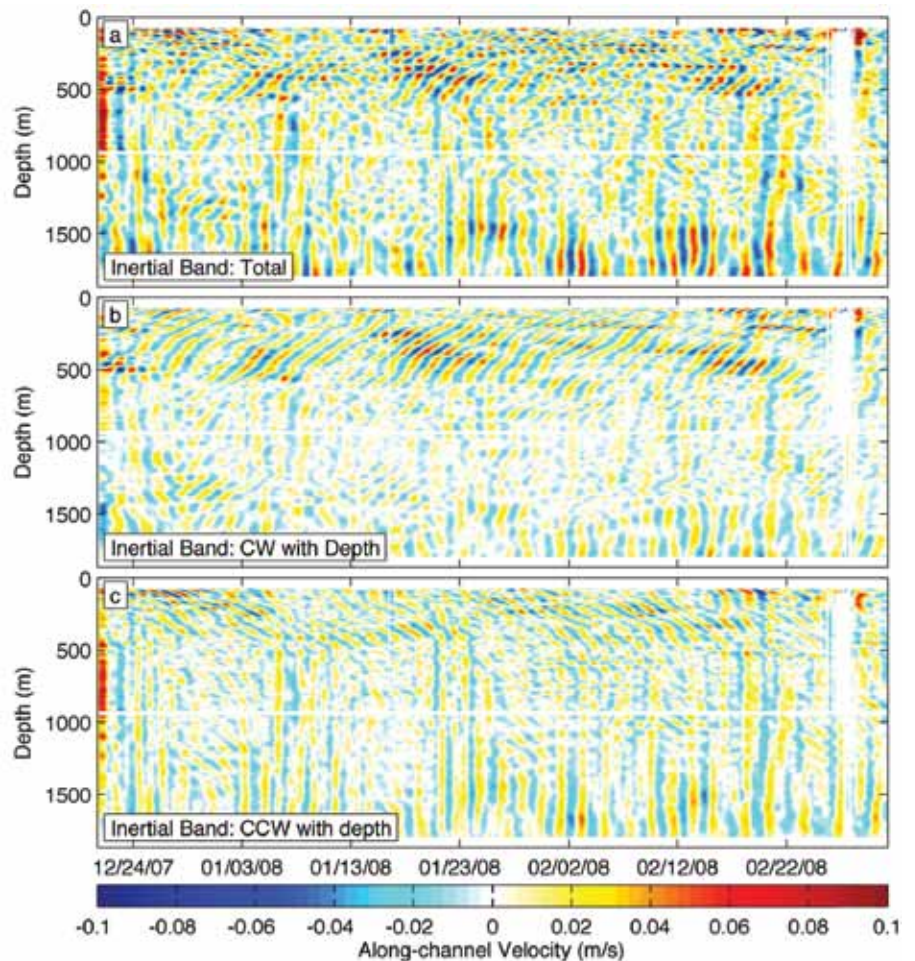


Figure 4. (a) Near-inertial bandpassed currents at MP1. (b) Reconstructed along-channel velocity from only the clockwise-with-depth portion of the rotary wavenumber spectrum of near-inertial currents (i.e., the part containing downward-propagating internal waves). (c) Same as (b) but using the counterclockwise-with-depth component (upward-propagating waves).

separated using rotary wavenumber spectra in panels 4b and 4c. Note that, because of the unique properties of internal waves, upward-sloping lines in Figure 4b indicate downward-propagating internal wave energy.

“ ...INTERNAL-WAVE-PERMITTING MODELS MUST BE ABLE TO REPRODUCE THE CONTRASTS BETWEEN THE LOW- AND HIGH-AMPLITUDE REGIMES SEEN IN OUR DATA SET. ”

The deeper layer of near-inertial band currents at MP1 (near the bottom at 1500–1800 m) has somewhat different characteristics, though also including a low-frequency modulation. Rather than rotating clockwise in time, these currents are nearly linearly polarized (as seen by the nearly equal levels at + 0.5 and - 0.5 cycles/day in Figure 2b at this depth). The rotary decomposition with depth indicates that this deep energy is mostly upward propagating (Figure 4c) and of fairly large vertical scale.

Wind Forcing

When considering what phenomena give rise to the velocity fluctuations seen by the moorings, two obvious candidates are wind and tides, both of which can force variability in the internal wave frequency range. Variations in wind speed and direction can, of course, occur at all frequencies, but the largest tend to be on synoptic (2–10 day) and longer time scales. In much of the world’s ocean,

the most direct influence of the winds on internal waves is through fluctuations near the inertial frequency (i.e., periods of two to three days at the latitude of the Philippines), forcing mixed-layer oscillations that radiate into the interior

as near-inertial waves (Alford, 2001). The very strongest near-inertial motions have been observed in the open ocean under forcing by strong, fast-moving storms with clockwise-rotating winds nearly in resonance with inertial motions (e.g., Sanford et al., 2007).

The bandpassed time series from MP1 (Figure 4), however, shows several obvious inconsistencies between the observed near-inertial waves and a wind-forcing mechanism. For one thing, the near-surface motions are relatively weak and not directly connected to those at intermediate depth, as they ought to be if wave radiation is occurring. For another, the vertical phase propagation (opposite the direction of internal wave energy propagation) is not exclusively upwards but contains hints of a “zigzag” or “checkerboard” pattern indicative of standing waves (or simultaneous upward and downward propagation) as seen by Alford et al. (2007). Finally, the presence of simultaneous near-inertial variability near the bottom and in the upper-mid

water column with little energy in between is also not suggestive of a surface source and vertical propagation.

To test the direct wind influence on internal waves, we have used a simple “slab” model of the upper ocean (Pollard and Millard, 1970; D’Asaro, 1985) forced by a high-frequency (hourly resolution) wind time series from the Coupled Ocean/Atmosphere Mesoscale Prediction System (COAMPS) model (Pullen et al., 2008) over the mooring deployment period and assuming a nominal mixed-layer depth for the region. This analysis yields both the mixed-layer currents and the integrated wind-work on the ocean (Alford, 2003). The wind-work (shown in Figure 5) is noteworthy in terms of its implications for the types of spatial patterns to look for in wind-generated internal waves, but is it applicable to near-inertial variability in the Philippines? Almost certainly so for the open basins and seas, but perhaps not for the straits. Interestingly enough, the most salient feature on the wind-work map is a swath of energy between 12° and 13°N that was produced by a single strong storm passing through the region (albeit significantly weaker than the one observed by Sanford et al. [2007]). In addition, there are hints of topographic shadowing and acceleration effects downwind (as this was the northeast monsoon period) of several islands. However, the time series of predicted currents (not shown) bears little resemblance to the mixed-layer currents observed at the moorings that showed, for example, minimal near-inertial enhancement following the storm passage on January 21 (Figure 4a,b). Instead, the observations indicate a fortnightly modulation of the

near-inertial band, closely following that of the diurnal tide but leading by about two days. Thus, while it is likely that near-inertial motions in the Pacific Ocean and South China Sea follow a forcing function similar to Figure 5, the internal wave climate in the straits must be explained by an alternate mechanism.

Tidal Forcing

Both diurnal and semidiurnal barotropic tides are significant in the Philippine Archipelago, with a broad spatial shift in dominance from semidiurnal in the Pacific Ocean to diurnal in the South China Sea. In addition to being more diurnal, the tidal amplitudes are also stronger in the SCS, and the greater tidal amplitudes at MP1 are likely a result of them. The energy pathway from the barotropic tide to the internal tide involves a conversion process, with flow over topography exchanging horizontal kinetic energy for vertical potential energy via work done against the background stratification. To illustrate the geography of this conversion, Figure 6 shows a map of the vertical velocity induced by the diurnal tide derived from the TPXO.7 tide model (Egbert and Erofeeva, 2002) and the best-available bathymetric slope from the SRTM30_PLUS data set. Though not an entirely reliable prediction of internal tides, due to the still-incomplete bathymetry data set and the tendency for constricted topography to cause departures from the open-ocean tidal currents, this map does give an indication of where the expected hot spots of internal tide generation might lie. Indeed, two well-known generation sites (Luzon Strait in the northern SCS and Sibutu Passage in the southern Sulu Sea) contain large values of this forcing

term. Models have predicted strong internal tides in these locations (Zhang et al., 2010), and in situ and remote-sensing observations have shown both linear internal tides and nonlinear waves radiating from these sites, emphasizing their extreme nature. Close to Mindoro Strait, the larger regions of generation appear to be in the SCS rather than in the Sulu Sea, with the straits themselves also containing numerous features with large tidal forcing (Figure 6b). Because internal tides have been observed to propagate long distances across the ocean (Alford, 2003; Zhao et al., 2010), it is quite possible that the internal tide observed at MP1 includes remote sources as far away as Luzon Strait.

Parametric Subharmonic Instability

With the elimination of wind forcing as a candidate for the generation of the near-inertial waves observed by the moorings, other options must be considered. For starters, inertial motions are a natural response of the rotating ocean to nearly any kind of impulsive forcing, including, potentially, baroclinic instability, geostrophic adjustment of a current to sharp channel curvature, or density perturbations induced by surface fluxes.

The close resemblance between the low-frequency modulation of the near-inertial waves (Figure 3) and that of the diurnal internal tide suggests that a connection between the two may be

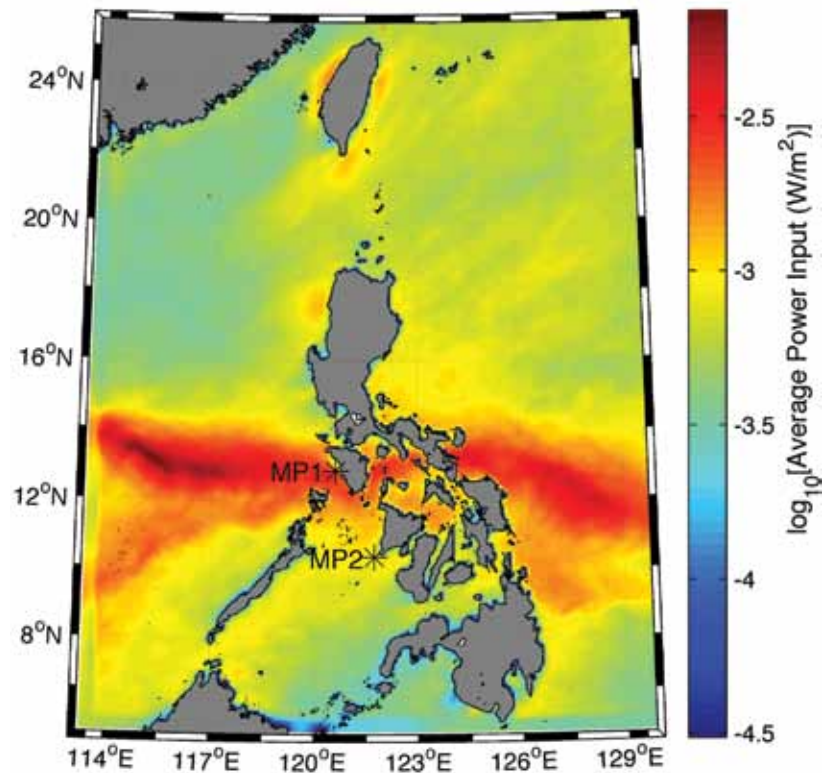


Figure 5. Average wind-energy input to near-inertial internal waves, computed using the damped slab model of Pollard and Millard (1970) and Coupled Ocean/Atmosphere Mesoscale Prediction System (COAMPS) winds (Pullen et al., 2008) over the two months of the mooring deployments (December 2007–February 2008).

active. Because the spring-neap modulation is a well-known property of the astronomical forcing, it appears likely that the near-inertial waves also have a tidal source. But how, if the inertial frequency is so different from the tidal?

The answer may come from a nonlinear wave-wave interaction process called parametric subharmonic instability (PSI). PSI is the breakdown of an internal wave into motions with half the frequency, and involves the enhancement of small perturbations in the flow by the advecting velocity field of the original wave. As such, its strength depends on the wave amplitude, which is largest (at least in velocity) where stratification is strong. A typical signature is the production of matched

upward- and downward-propagating pairs of waves, forming a “resonant triad.” In order for the resulting motions to be internal waves, this resonant triad must occur equatorward of the critical latitude where the tide is twice the inertial frequency (i.e., 14.5°N for the diurnal K1 tide with a period of 24.03 h). Just as wind-forced inertial waves are strongest when the wind varies in resonance with the inertial frequency motions, PSI is strongest close to this critical latitude (MacKinnon and Winters, 2005; Alford, 2008). Thus, because (a) diurnal internal tides are strong at MP1, (b) the observed near-inertial waves bear little resemblance to the periods of enhanced wind forcing, and (c) the Philippine seas lie not far south of the K1 critical

latitude, PSI is a likely candidate for the fortnightly modulation of the near-inertial internal waves.

CONCLUSIONS

We clearly see that both internal tides and near-inertial waves have unique characteristics in the Philippine Archipelago, requiring both attention in archipelago modeling and future exploration of mechanisms. At a most basic level, the fact that the velocities of the internal tide are comparable to or greater than those of the barotropic tide means that direct comparisons between modeled and observed surface currents will be suspect until realistic internal tides can be simulated. In addition, the enhancement of near-bottom shear,

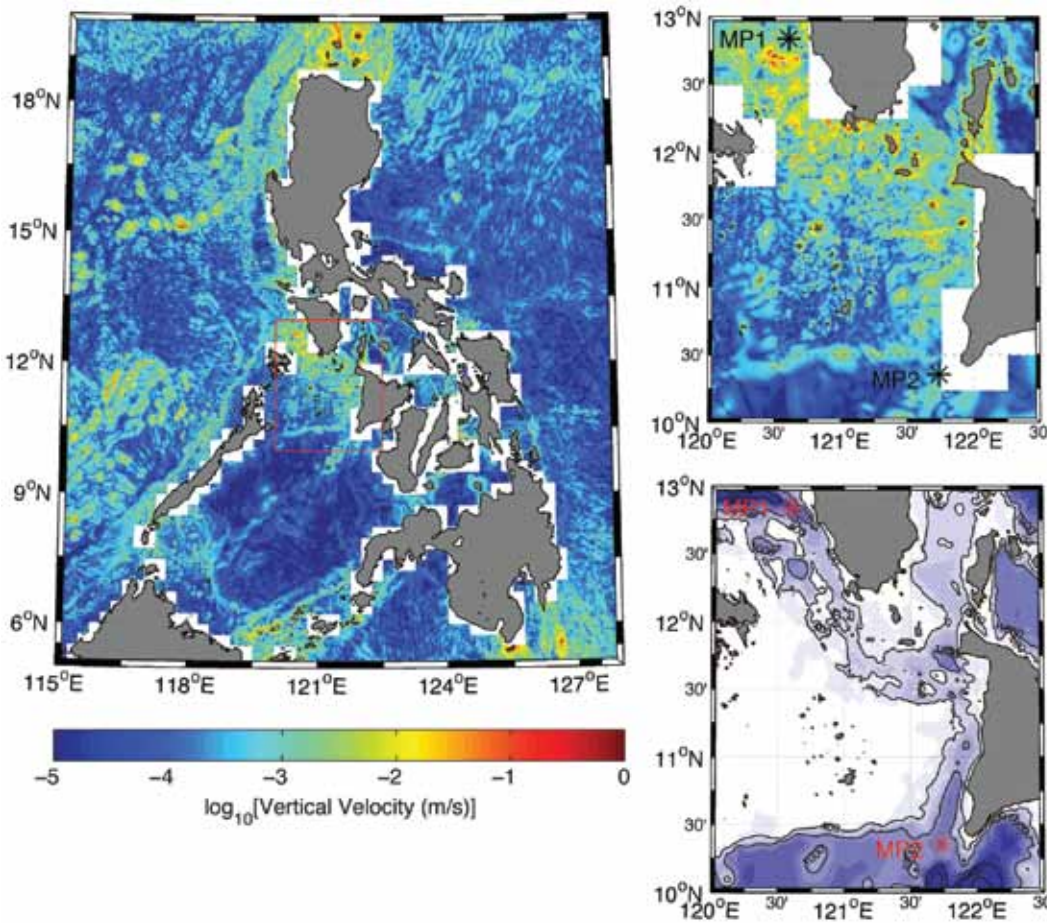


Figure 6. (left) Forcing of diurnal (K1) internal waves by tidal flow over topography, estimated from TPXO.7 currents (Egbert and Erofeeva, 2002) and SRTM30_PLUS bottom slope (Becker et al., 2009). The quantity plotted is the logarithm of the induced near-bottom vertical velocity amplitude (Bell, 1975). (right) Magnified views of the tidal forcing and bathymetry in the Mindoro-Tablas junction or “mixing bowl.” Though a continuous channel does exist, the multitude of seamounts and islands provides much potential for internal tide generation. In particular, the Apo Reef, just south of mooring location MP1, is likely to be a strong generation site.


dissipation by topographic focusing of internal tides, and the domination of near-inertial internal waves in mid-depth shear emphasize the importance of these types of internal waves in mixing and water mass modification during transit through the archipelago.

At the high-energy end of the range, the reduction of salinity extrema along the path from the South China Sea to the Sulu Sea points to a significant role for internal wave mixing in the Mindoro-Tablas junction. Both steepening incoming internal tides (and conversion to near-inertial waves through PSI) and local waves from the multitude of nearby generation sites contribute to this mixing. At the low-energy end, reduced levels of oxygen in the deep Sibuyan Sea are a result of long residence times and low levels of internal waves. Though the sea itself is quite deep, the shallow sills and weak tides around the boundaries effectively cut it off from remote internal wave sources.

At a minimum, internal-wave-permitting models must be able to reproduce the contrasts between the low- and high-amplitude regimes seen in our data set. Alternatively, the quasi-static nature of many of these contrasts suggests that suitably calibrated mixing parameterizations could be developed involving a combination of (a) the distribution of internal tide generation sites, (b) wind forcing over open waters, (c) wave propagation and reflection to allow for remote influences and topographic shielding, and (d) PSI.

ACKNOWLEDGEMENTS

This work was supported by the Office of Naval Research under grants N00014-06-1-0685 and N00014-07-1-0927. The

design, construction, and deployment of the moorings would not have been possible without the able assistance of John Mickett, Eric Boget, Paul Aguilar, Andrew Cookson, and the captain and crew of R/V *Melville*. 

REFERENCES

- Alford, M.H. 2001. Internal swell generation: The spatial distribution of energy flux from the wind to mixed layer near-inertial motions. *Journal of Physical Oceanography* 31:2,359–2,368.
- Alford, M. 2003. Improved global maps and 54-year history of wind-work on ocean inertial motions. *Geophysical Research Letters* 30(8), 1424, doi:10.1029/2002GL016614.
- Alford, M.H. 2008. Observations of parametric subharmonic instability of the diurnal internal tide in the South China Sea. *Geophysical Research Letters* 35, L15602, doi:10.1029/2008GL034720.
- Alford, M.H., J.A. MacKinnon, Z. Zhao, R. Pinkel, J. Klymak, and T. Peacock. 2007. Internal waves across the Pacific. *Geophysical Research Letters* 34, L24601, doi:10.1029/2007GL031566.
- Arango, H.G., J.C. Levin, E.N. Curchitser, B. Zhang, A.M. Moore, W. Han, A.L. Gordon, C.M. Lee, and J.B. Girton. 2011. Development of a hindcast/forecast model for the Philippine Archipelago. *Oceanography* 24(1):58–69.
- Becker, J.J., D.T. Sandwell, W.H.F. Smith, J. Braud, B. Binder, J. Depner, D. Fabre, J. Factor, S. Ingalls, S-H. Kim, and others. 2009. Global bathymetry and elevation data at 30 arc seconds resolution: SRTM30 PLUS. *Marine Geodesy* 32:355–371.
- Bell, T.H. Jr. 1975. Topographically generated internal waves in the open ocean. *Journal of Geophysical Research* 80:320–327.
- D'Asaro, E. 1985. The energy flux from the wind to near-inertial motions in the mixed layer. *Journal of Physical Oceanography* 15:943–959.
- Egbert, G., and S. Erofeeva. 2002. Efficient inverse modeling of barotropic ocean tides. *Journal of Atmospheric and Oceanic Technology* 19:183–204, 2002.
- Garrett, C.J.R., and W.H. Munk. 1975. Space-time scales of internal waves: A progress report. *Journal of Geophysical Research* 80:291–297.
- Hurlburt, H.E., E.J. Metzger, J. Sprintall, S.N. Riedlinger, R.A. Arnone, T. Shinoda, and X. Xu. 2011. Circulation in the Philippine Archipelago simulated by 1/12° and 1/25° global HYCOM and EAS NCOM. *Oceanography* 24(1):28–47.
- Jackson, C.R., Y. Arvelyna, and I. Asanuma. 2011. High-frequency nonlinear internal waves around the Philippines. *Oceanography* 24(1):90–99.
- Lermusiaux, P.F.J., P.J. Haley Jr., W.G. Leslie, A. Agarwal, O.G. Logutov, and L.J. Burton. 2011. Multiscale physical and biological dynamics in the Philippine Archipelago: Predictions and processes. *Oceanography* 24(1):70–89.
- MacKinnon, J.A., and K.B. Winters. 2005. Subtropical catastrophe: Significant loss of low-mode tidal energy at 28.9°. *Geophysical Research Letters* 32, L15605, doi:10.1029/2005GL023376.
- May, P.W., J.D. Doyle, J.D. Pullen, and L.T. David. 2011. Two-way coupled atmosphere-ocean modeling of the PhilEx Intensive Observational Periods. *Oceanography* 24(1):48–57.
- Pollard, R., and R. Millard. 1970. Comparison between observed and simulated wind-generated inertial oscillations. *Deep-Sea Research* 17:813–816.
- Pullen, J., J. Doyle, P. May, C. Chavanne, P. Flament, and R. Arnone. 2008. Monsoon surges trigger oceanic eddy formation and propagation in the lee of the Philippine Islands. *Geophysical Research Letters* 35, L07604, doi:10.1029/2007GL033109.
- Sanford, T., J. Price, J. Girton, and D. Webb. 2007. Highly resolved observations and simulations of the ocean response to a hurricane. *Geophysical Research Letters* 34, L13604, doi:10.1029/2007GL029679.
- Zhang, B., E. Curchitser, J. Levin, H. Arango, and W. Han. 2011. Modeling the internal tides and energy flux in the Sulu Sea and adjacent area. *Journal of Geophysical Research*, submitted.
- Zhao, Z., and M.H. Alford. 2006. Source and propagation of internal solitary waves in the northeastern South China Sea. *Journal of Geophysical Research* 111, C11012, doi:10.1029/2006JC003644.
- Zhao, Z., M.H. Alford, J.A. MacKinnon, and R. Pinkel. 2010. Long-range propagation of the semidiurnal internal tide from the Hawaiian Ridge. *Journal of Physical Oceanography* 40:713–736.